Revisiting Mott's model for the thermopower of Pd_xAg_{1-x} alloys with support of density functional theory

Maximilien Saint-Cricq, Natalio Mingo, and Ambroise van Roekeghem*
Université Grenoble Alpes, CEA, LITEN, 17 Rue des Martyrs, 38054 Grenoble, France

(Received 14 February 2022; revised 6 May 2022; accepted 6 May 2022; published 20 May 2022)

Electronic properties of palladium-silver alloys have been studied for almost a century as a prototype of a transition-metal alloy with entangled *s* and *d* bands. We review the literature starting from Mott's model of 1935 and discuss from a quantitative point of view a series of common assumptions stemming from that seminal paper. We also show that spectral functions obtained by unfolding the band structures of a sample of supercells can be used for the *ab initio* computation of the thermopower of such systems within a Boltzmann transport equation approach.

DOI: 10.1103/PhysRevB.105.195128

I. INTRODUCTION

The transport properties of late transition-metal alloys were studied by Mott in a series of papers in the years 1935–1936 [1–3] in the framework of the so-called *s*-*d* model. In this model, it is postulated that the electrical conduction is essentially due to the free-electron-like *s* band, which has a lighter mass than the *d* bands, but that conduction is limited by the scattering of these electrons from the *s* band to the partially filled *d* bands with a high density of states (DOS). Furthermore, alloys were considered in a rigid-band picture [4] as pure metals with a certain amount of doping.

In this context, Mott proposed an explanation for the shape of the curve of the thermopower of the palladium-silver and palladium-gold alloys, which presents a marked peak around 55 atomic percent of the noble metal. Since the DOS of the *s* band is almost constant within the energy scale relevant for transport (as illustrated on Fig. 1), the variation of the thermopower is attributed entirely to the variation of the lifetime of the *s* electrons with energy, with a scattering rate proportional to the *d*-electrons DOS. With the approximation of a parabolic dispersion, the peak of the thermopower is obtained when the *d* bands become filled, close to the 50-50 alloy composition. In the Ag-rich side, the thermopower is found constant and equal to that of pure Ag, while in the Pd-rich side its absolute value decreases progressively towards that of pure Pd.

An attempt to quantitatively assess the hypotheses of Mott's model was made by Coles and Taylor in 1962 [5] by combining specific-heat and resistivity measurements. They obtained good overall agreement between the model and the experimental curves but already pointed out a possible contribution of the *d* holes to transport on the Pd-rich side. In the same line, Dugdale and Guénault [6] proposed a model with split *d* bands for Pd and Ag and attempted to explain the shape of the thermopower on the Ag-rich side by a modification of the position of the Pd-*d* bands with composition.

Forty-five years after its first formulation, Mott's theory was still the baseline model to explain the transport properties of transition-metal alloys. In the early 80s, the developments of density-functional theory (DFT) and of the coherent potential approximation (CPA) finally allowed to assess some of its assumptions [7]. Several studies have reported the calculation of the electronic properties of Pd_xAg_{1-x} alloys within the CPA as a typical benchmark (see, for instance, Refs. [7–13]). In this line, the series of Refs. [8–10] present the most exhaustive discussion on the transport properties, including some critical comparison with the Mott model. In particular, these studies point out that the Pd and Ag bands can be split—although the successive publications appear contradictory on this aspect, that the so-called *s* band with high group velocity actually also has substantial *d*-orbital character, and that the scattering rates are not proportional to the DOS.

In this study, we adopt a quasiparticle point of view to reexamine the electronic structure and the thermopower of Pd_xAg_{1-x} alloys from a simple perspective. Our main finding is that the *d* holes make an important contribution to the thermopower, in contrast with the original hypothesis of Mott, which was not really contradicted by the next studies. We also take this opportunity to benchmark a method to calculate the thermopower based on the Boltzmann transport equation with electrons energies and lifetimes extracted from unfolded spectral functions.

II. ELECTRONIC STRUCTURE OF Pd_xAg_{1-x}

We begin by displaying in Fig. 1 the band structure and DOS of pure Pd, as computed with the VASP code [14] within the local density approximation (LDA), and plotted with SUMO-BANDPLOT [15]. The lattice parameter is 3.892 Å, as obtained using the QSCAILD code [16], including thermal expansion at 1000 K. For pure Ag we obtain a lattice parameter of 4.073 Å at 1000 K, and we use Vegard's law in the case of alloys. The obtained orbital characters show a strongly dispersive hybridized *spd* band with a bottom around −7.3eV and a bandwidth of the order of 16 eV, entangled with the 4*d* manifold which lies between about −5.5 and 0.3 eV. The DOS

*ambroise.vanroekeghem@cea.fr

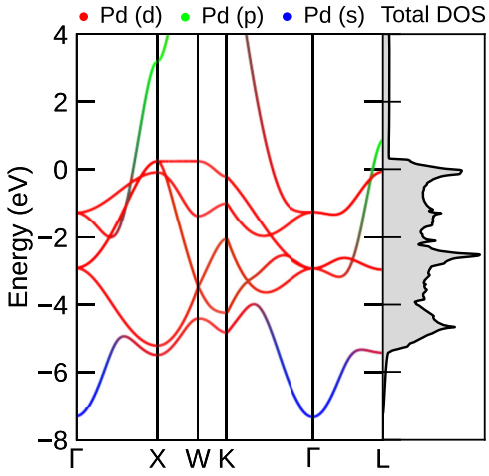

FIG. 1. Band structure with orbital characters of pure Pd, and total density of states.

of the dispersive band is negligible compared with that of the d manifold in the energy range in which they overlap. At this point, we already note that the hypothesis that the contribution of d electrons can be neglected due to their large effective mass is doubtful, since this small group velocity is also at the origin of a high DOS.

This first impression is confirmed by inspecting the evolution of the Fermi surface as a function of alloy composition, shown in Fig. 2 in the virtual crystal approximation (VCA) [17,18]. In the limit of constant mean-free path, the thermopower is proportional to the derivative of the area of the Fermi surface with respect to the Fermi level [19], which in our case is comparable to its evolution as a function of silver content. On the Ag-rich side, we observe a single electron pocket due to the *spd* band, which will provide a negative contribution to the thermopower (brown Fermi surface in Fig. 2). On the Pd-rich side, the Fermi surface is much more complex but is composed of two contributions: the same electron pocket (brown), and several hole pockets (violet and red surfaces on Fig. 2) due to d bands, which will be responsible for a strong positive contribution to the thermopower since their areas varies rapidly. This positive contribution disappears around $x = 0.6$ in Pd_xAg_{1-x}, which corresponds to the minimum of the alloy thermopower. In the following, we show that the hole contribution from the d electrons is indeed not negligible, although it is reduced by their shorter lifetimes.

III. SCATTERING BY IMPURITIES AND PHONONS

To assess alloy scattering effects on the electronic structure, we use the following approach. For each composition, a sample of 100 $4 \times 4 \times 4$ supercells (64 atoms) is constructed, with a random distribution of Pd and Ag atoms corresponding to the alloy composition. The electronic structure in the LDA is then computed on a grid of $11 \times 11 \times 11$ wave vector points, with a Fermi smearing corresponding to 1000 K, and unfolded to a $44 \times 44 \times 44$ grid of the primitive Brillouin zone using the BANDUP code [20,21]. The average of these unfolded spectra over all configurations, with aligned Fermi levels, is interpreted as a spectral function. At each wave vector we fit this spectral function to a sum of Lorentzians of unit weight corresponding to the total number of bands of the VCA band structure in the fitted energy window. We use the *lmfit* Python package, with the VCA eigenenergies as starting point. The obtained peak centers and widths at half maximum are then interpreted as quasiparticle energies and scattering rates, which we use to compute the thermopower with the BoltzTraP2 code with interpolation on a ten-times denser wave vector grid [22].

We include electron-phonon scattering in the pure Pd and Ag compounds via a similar procedure: a spectral function is produced as before, but using the sampling of atomic positions implemented in QSCAILD and the self-consistent interatomic force constants at 1000 K. In other cases, we included only alloy scattering. We also note that relaxing atomic positions in the alloy supercells had a negligible impact on the result, as tested on one composition.

The interpretation of unfolded band structures as spectral functions and its implications has been described by several authors, both in the context of alloys and of electron-phonon scattering (see, for instance, Refs. [23–30]). In principle, our stochastic sampling method might be improved by using special quasirandom structures [31] and special displacements for phonons [28]. On the other hand, the fit with Lorentzian lines requires sufficient statistics of the whole distribution in energy, which is provided by this stochastic sampling. We also note that the obtained lineshapes are actually different from Lorentzians—notably, the energy distributions typically present an asymmetry—but we nevertheless make this approximation for simplicity and robustness. To our knowledge, such a systematic extraction of lifetimes on the whole Brillouin zone to compute transport properties has not been exploited yet on spectral functions from unfolded band structures. However, we note that a similar fitting procedure was used on CPA-based spectral functions in Ref. [10]. A further improvement could be, for instance, to use statistical sampling techniques to reflect clustering in the generation of the supercell configurations.

Figure 3 displays such spectral functions for the cases of pure Pd and of $Pd_{0.6}Ag_{0.4}$. The orbital and momentum dependence of scattering appears qualitatively similar in both cases, with much stronger scattering on the d orbitals than on s and p orbitals. The spectral function of the analog $Cu_{0.6}Ni_{0.4}$ as computed within the CPA in Ref. [32] also displays similar

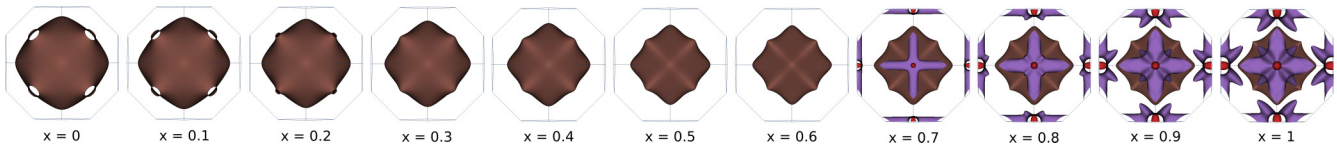

FIG. 2. Fermi surface of Pd_xAg_{1-x} in the virtual crystal approximation at 0 K.

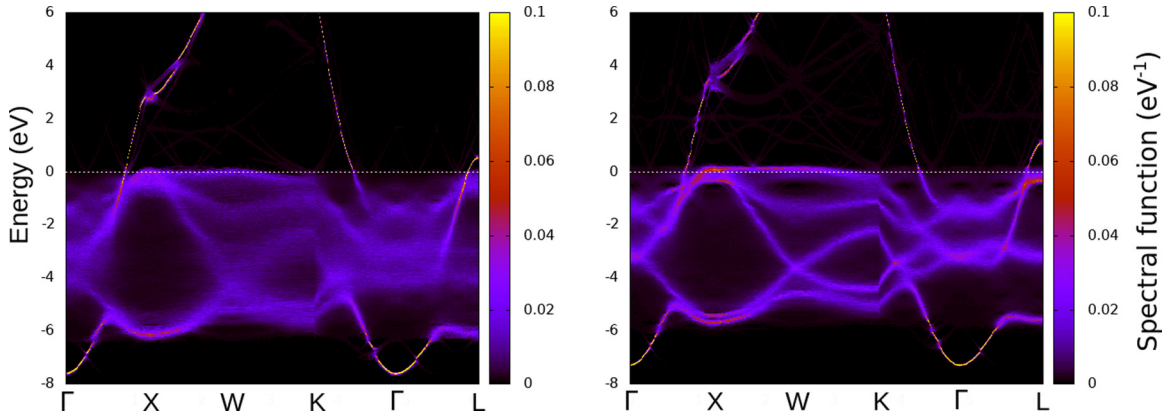

FIG. 3. Spectral functions of $Pd_{0.6}Ag_{0.4}$ (left) and of Pd (right) at 1000 K, along the Γ-X-W-K-Γ-L path and with energy bins of 10 meV. The Fermi level is indicated by a white dashed line.

features. In contrast with the analysis of Ref. [8], which insisted on the splitting of Pd and Ag d bands, we treated the whole band structure as in the VCA. Indeed, in most of the Brillouin zone—and in particular close to the Fermi level—Pd and Ag appear to form common bands, although a signature of split bands can be noted, for instance, at the L point around −4 eV. In the original Mott papers, s-s and s-d scattering were considered to be mediated either by lattice vibrations or by impurity scattering. Indeed, both can be considered as a perturbation of the local potential around the equilibrium atomic positions. In this context, it is expected that the longer-range, more delocalized band experiences less scattering than the more localized d orbitals. This lifetime effect should thus reduce the positive contribution to the thermopower from the d bands in the Pd-rich side with respect to the negative contribution.

We verify this effect in Fig. 4, which displays the lifetimes obtained as $\tau = \hbar/\Delta E$, with ΔE being the full widths at half maximum of the fitted Lorentzians. We observe that the lifetimes are momentum dependent, and that when both the d and the spd pockets are present the lifetimes of carriers on the d pocket are indeed smaller—typically by a factor of 2–3. Two effects are acting on the lifetimes: modification of the total electron filling, and modification of the scattering potential. As expected, the compounds with lowest alloying content have longer lifetimes on all pockets. In those cases of low alloying, we note that neglecting electron-phonon scattering at 1000 K can be disputable, especially on the Pd-rich side.

IV. THERMOPOWER

Figure 5 displays the computed thermopower within the Boltzmann picture and the constant relaxation time approximation (CRTA), as well as with a lifetime inversely proportional to the DOS. The latter is comparable to, although different from, Mott's model: in the original paper, different amplitudes were introduced for the scattering to s or to d states—while we make no distinction here—and the contribution of holes was neglected—while it is included here. Finally, we also show the computed values with a lifetime obtained from the spectral functions as discussed above. As can be seen from the CRTA result, the contribution of hole pockets in the Pd-rich side is strong despite their high effective mass, giving a total maximum positive value for pure Pd of about 23 $\mu V\,K^{-1}$. Lifetime effects caused by electron-phonon scattering strongly reduce it such that the thermopower becomes about -41 $\mu V\,K^{-1}$. Overall, the thermopower computed based on the spectral functions presents good agreement with the experiment, while the model with scattering rates proportional to the DOS appears to overestimate lifetime effects on the Pd-rich side, and underestimate them on the Ag-rich side. The position of the peak of the thermopower is also different: while in the CRTA the thermopower starts to increase as soon as the d bands are partially emptied—around $x = 0.5$ at 1000 K—the peak of the $\tau \propto 1/\mathrm{DOS}$ approximation is observed around $x = 0.8$ due to the precise shape of the d-band DOS. The experimental peak is in-between those two model situations at $x = 0.6$, as is the peak of our calculation at $x = 0.7$, which is consistent with a combined effect of the hole contribution from the d bands and of an evolution of the scattering rates that is only partly driven by the DOS.

The main discrepancy between our calculations and experimental values appears for pure Ag, with a difference of sign similar to that of the CRTA. This sign difference was explained by lifetime effects due to electron-phonon coupling in Refs. [34,35]. We suspect that this deviation is linked to the difficulty of sampling correctly the variations of the scattering rates in the strongly dispersive band with long lifetimes, which

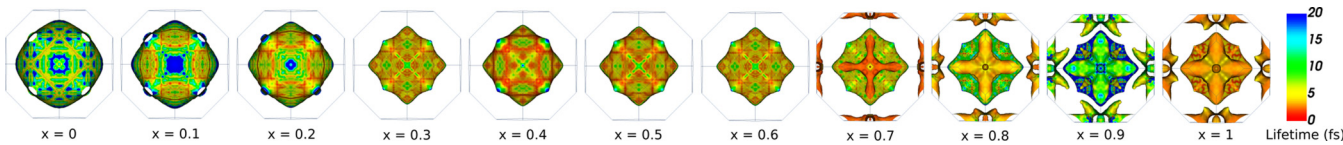

FIG. 4. Carrier lifetimes on the Fermi surfaces of Pd_xAg_{1-x} due to electron-phonon scattering at 1000 K for the pure compounds and only to alloy scattering in other cases.

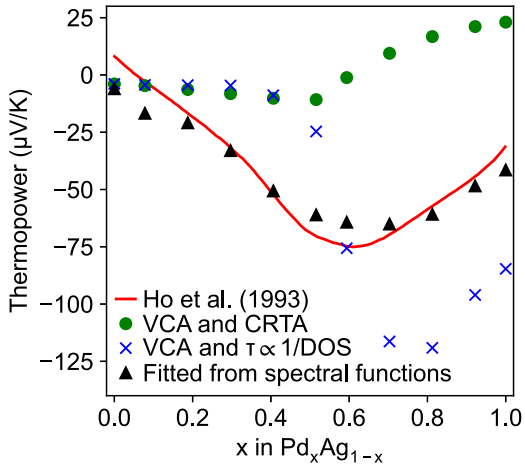

FIG. 5. Thermopower of Pd_xAg_{1-x} at 1000 K as computed using the virtual crystal and constant relaxation-time approximations (green dots), with a scattering rate proportional to the DOS (blue crosses), and using energies and lifetimes extracted from the spectral functions (black triangles). We also show reference experimental values from Ref. [33] (red line).

requires a very tight wave vector and energy grids, and high statistics. In contrast, for pure Pd the effects of electron-phonon scattering are satisfyingly captured.

Another interesting aspect is the overall trend in the Ag-rich side, in which a model of scattering proportional to the DOS does not explain the strong negative thermopower compared with the CRTA result—which was to be expected, since in this case the DOS close to the Fermi level is nearly constant. Based on the linewidths of the spectral functions of Fig. 3 and on the orbital characters of Fig. 1, we attribute this difference to a decrease of the lifetime of the dispersive *spd* band when approaching the 4*d* manifold, due to its increasing *d*-orbital character.

V. CONCLUSION

In conclusion, we have reviewed in detail the different contributions of the electronic structure to the thermopower of Pd_xAg_{1-x} compounds. We have shown that the contribution from the holes in the 4*d* manifold is not negligible in the Pd-rich side, and that the *d*-orbital character of the *spd* band also drives the behavior of the thermopower on the Ag-rich side. Finally, we have demonstrated how unfolded spectral functions can be used to compute transport properties in the Boltzmann picture in such systems by providing good estimates of scattering effects due to impurity or electron-phonon interactions.

ACKNOWLEDGMENT

We acknowledge support from the APERAM company.

[1] N. F. Mott, A discussion of the transition metals on the basis of quantum mechanics, Proc. Phys. Soc. **47**, 571 (1935).
[2] N. F. Mott, The electrical conductivity of transition metals, Proc. R. Soc. London, Ser. A **153**, 699 (1936).
[3] N. F. Mott, The resistance and thermoelectric properties of the transition metals, Proc. R. Soc. London, Ser. A **156**, 368 (1936).
[4] N. Mott and H. Jones, *The Theory of the Properties of Metals and Alloys*, The International Series of Monographs on Physics (Clarendon Press, Oxford, 1936).
[5] B. R. Coles, J. C. Taylor, and H. Jones, The electrical resistivities of the palladium-silver alloys, Proc. R. Soc. London, Ser. A **267**, 139 (1962).
[6] J. S. Dugdale and A. M. Guénault, The low temperature transport properties of the palladium-silver alloy series, Philos. Mag. (1798–1977) **13**, 503 (1966).
[7] H. Winter and G. M. Stocks, Calculation of self-consistent potentials for substitutionally disordered systems with application to the $Ag_x - Pd_{1-x}$ alloy series, Phys. Rev. B **27**, 882 (1983).
[8] A. J. Pindor, W. M. Temmerman, B. L. Gyorffy, and G. M. Stocks, On the electronic structure of Ag_cPd_{1-c} alloys, J. Phys. F: Met. Phys. **10**, 2617 (1980).
[9] G. M. Stocks and W. H. Butler, Mass and Lifetime Enhancement Due to Disorder on Ag_cPd_{1-c} Alloys, Phys. Rev. Lett. **48**, 55 (1982).
[10] W. H. Butler and G. M. Stocks, Calculated electrical conductivity and thermopower of silver-palladium alloys, Phys. Rev. B **29**, 4217 (1984).
[11] P. M. Laufer and D. A. Papaconstantopoulos, Tight-binding coherent-potential-approximation study of the electronic states of palladium–noble-metal alloys, Phys. Rev. B **35**, 9019 (1987).
[12] J. Banhart and H. Ebert, First-principles calculation of the thermoelectric power of disordered alloys, Solid State Commun. **94**, 445 (1995).
[13] M. Oshita, S. Yotsuhashi, H. Adachi, and H. Akai, Seebeck coefficient calculated by Kubo-Greenwood formula on the basis of density functional theory, J. Phys. Soc. Jpn. **78**, 024708 (2009).
[14] G. Kresse and J. Furthmüller, Efficiency of ab-initio total energy calculations for metals and semiconductors using a plane-wave basis set, Comput. Mater. Sci. **6**, 15 (1996).
[15] A. M. Ganose, A. J. Jackson, and D. O. Scanlon, Sumo: Command-line tools for plotting and analysis of periodic *ab initio* calculations, J. Open Source Software **3**, 717 (2018).
[16] A. van Roekeghem, J. Carrete, and N. Mingo, Quantum self-consistent ab-initio lattice dynamics, Comput. Phys. Commun. **263**, 107945 (2021).
[17] L. Bellaiche and D. Vanderbilt, Virtual crystal approximation revisited: Application to dielectric and piezoelectric properties of perovskites, Phys. Rev. B **61**, 7877 (2000).
[18] C. Eckhardt, K. Hummer, and G. Kresse, Indirect-to-direct gap transition in strained and unstrained Sn_xGe_{1-x} alloys, Phys. Rev. B **89**, 165201 (2014).
[19] J. M. Ziman, *Electrons and Phonons* (Clarendon Press, Oxford, 1960).
[20] P. V. C. Medeiros, S. Stafström, and J. Björk, Effects of extrinsic and intrinsic perturbations on the electronic structure of

graphene: Retaining an effective primitive cell band structure by band unfolding, Phys. Rev. B **89**, 041407(R) (2014).

[21] P. V. C. Medeiros, S. S. Tsirkin, S. Stafström, and J. Björk, Unfolding spinor wave functions and expectation values of general operators: Introducing the unfolding-density operator, Phys. Rev. B **91**, 041116(R) (2015).

[22] G. K. H. Madsen, J. Carrete, and M. J. Verstraete, BoltzTraP2, a program for interpolating band structures and calculating semi-classical transport coefficients, Comput. Phys. Commun. **231**, 140 (2018).

[23] W. Ku, T. Berlijn, and C.-C. Lee, Unfolding First-Principles Band Structures, Phys. Rev. Lett. **104**, 216401 (2010).

[24] V. Popescu and A. Zunger, Effective Band Structure of Random Alloys, Phys. Rev. Lett. **104**, 236403 (2010).

[25] Y. Zhang and L.-W. Wang, Global electronic structure of semiconductor alloys through direct large-scale computations for III-V alloys $Ga_xIn_{1-x}P$, Phys. Rev. B **83**, 165208 (2011).

[26] M. W. Haverkort, I. S. Elfimov, and G. A. Sawatzky, Electronic structure and self energies of randomly substituted solids using density functional theory and model calculations, arXiv:1109.4036.

[27] V. Popescu and A. Zunger, Extracting E versus $\vec{k}$ effective band structure from supercell calculations on alloys and impurities, Phys. Rev. B **85**, 085201 (2012).

[28] M. Zacharias and F. Giustino, Theory of the special displacement method for electronic structure calculations at finite temperature, Phys. Rev. Research **2**, 013357 (2020).

[29] F. C. Yang, O. Hellman, and B. Fultz, Temperature dependence of electron-phonon interactions in vanadium, Phys. Rev. B **101**, 094305 (2020).

[30] M. Zacharias, M. Scheffler, and C. Carbogno, Fully anharmonic nonperturbative theory of vibronically renormalized electronic band structures, Phys. Rev. B **102**, 045126 (2020).

[31] A. Zunger, S.-H. Wei, L. G. Ferreira, and J. E. Bernard, Special Quasirandom Structures, Phys. Rev. Lett. **65**, 353 (1990).

[32] B. Wiendlocha, Thermopower of thermoelectric materials with resonant levels: PbTe:Tl versus PbTe:Na and $Cu_{1-x}Ni_x$, Phys. Rev. B **97**, 205203 (2018).

[33] C. Ho, R. Bogaard, T. Chi, T. Havill, and H. James, Thermoelectric power of selected metals and binary alloy systems, Thermochim. Acta **218**, 29 (1993).

[34] S. Kou and H. Akai, First-principles calculation of transition-metal Seebeck coefficients, Solid State Commun. **276**, 1 (2018).

[35] B. Xu, M. Di Gennaro, and M. J. Verstraete, Thermoelectric properties of elemental metals from first-principles electron-phonon coupling, Phys. Rev. B **102**, 155128 (2020).